AD NUMBER
AD501322
CLASSIFICATION CHANGES
TO: **unclassified**
FROM: **confidential**
LIMITATION CHANGES
TO: **Approved for public release, distribution unlimited**
FROM: **Distribution: Further dissemination only as directed by Director, Naval Research Laboratory, Washington, DC 20390, 20 MAR 1969, or higher DoD authority.**
AUTHORITY
NRL Code/5309 memo dtd 20 Feb 1997; NRL Code/5309 memo dtd 20 Feb 1997

AD NUMBER

AD501322

CLASSIFICATION CHANGES

TO

confidential

FROM

secret

AUTHORITY

31 Mar 1981, per document marking, DoDD 5200.10

AD- 501322

SECURITY REMARKING REQUIREMENTS

DOD 5200.1-R, DEC 78

REVIEW ON 20 MAR 89

SECURITY MARKING

The classified or limited status of this report applies to each page, unless otherwise marked.
Separate page printouts MUST be marked accordingly.

SECRET

NRL Report 6866
Copy No.

Ionospheric Earth Backscatter Simulation Applied to Over-the-Horizon Radar

[Unclassified Title]

JOHN R. DAVIS, FRANK W. CHAMBERS, EDWIN L. ALTHOUSE, AND JOHN W. WILLIS

Radar Techniques Branch
Radar Division

March 20, 1969

SECRET

SECURITY

This document contains information affecting the national defense of the United States within the meaning of the Espionage Laws, Title 18, U.S.C., Sections 793 and 794. The transmission or revelation of its contents in any manner to an unauthorized person is prohibited by law.

In addition to security requirements which apply to this document and must be met, it may be further distributed by the holder *only* with specific prior approval of the Director, Naval Research Laboratory, Washington, D.C. 20390.

CONTENTS

ABSTRACT
(Secret)

A precision ionospheric ray-tracing technique has been developed to predict in detail the distribution of earth backscatter measured by a high-frequency over-the-horizon radar. A first-generation version of this technique was reported in NRL Report 6731. By making use of observed earth-backscatter distributions, in conjunction with ionospheric sounding data, it has been possible to refine the ray-tracing technique and improve its performance in predicting signatures of over-the-horizon rocket launches. In particular, it has been possible to predict the time of signature onset more precisely with these improvements.

This ray-tracing technique could be used in an operational over-the-horizon radar to provide, in near real time, estimates of trajectory parameters for actual hostile missile launches. Implementation of this capability in an operational radar would require the use of a sophisticated hybrid (digital/analog) computer as an integral part of the radar controller and signal processor.

PROBLEM STATUS

This is an interim report on one phase of a continuing problem. Work is proceeding on this and several allied subjects.

AUTHORIZATION

NRL Problem R02-23
USAF MIPR FD2310-7-0016

Manuscript submitted December 4, 1968.

49593

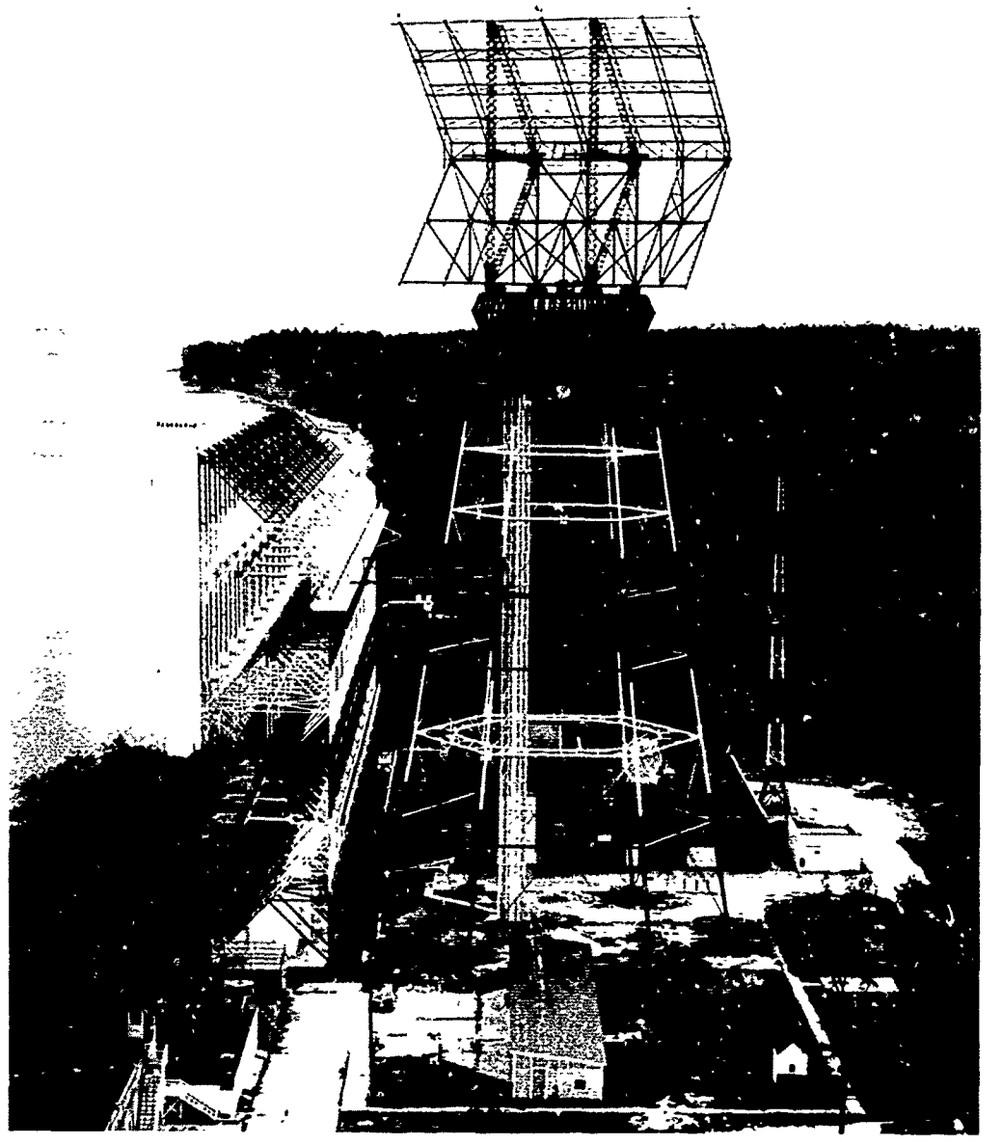

Fig. 1 - Elevated rotatable antenna for the Madre radar and a fixed broadside array for the Madre radar (S)

IONOSPHERIC EARTH BACKSCATTER SIMULATION APPLIED TO OVER-THE-HORIZON RADAR
[Unclassified Title]

INTRODUCTION (U)

The Madre Research Radar (S)

(S) The Madre research radar is an advanced, coherent-pulse-doppler ionospheric research device, which has been developed by NRL in a continuous evolution which began in the mid-1950's. At the early stages of its development this radar was used primarily for investigating whether sophisticated signal-storage and coherent bandwidth-narrowing could extract below-noise-level echoes from small, distant radar targets. Over-the-horizon radar was an obvious embodiment of these techniques, and shortly after its inception Madre was given the tasks of applying them to the detection of over-the-horizon rocket launches and high-altitude nuclear explosions as well as remote aircraft targets. Over the past decade the Madre research radar has grown and evolved in pursuit of these tasks, with advancements in signal-processing techniques introduced to cope with the increasing complexity of radar data from the accelerating, diffuse, often fleeting targets represented by these objects. Improvements in radio-frequency power transmission and hf antenna array design have also been incorporated in the Madre research radar during its growth. An extensive continuing program of experimental and theoretical research in ionospheric propagation has accompanied the development of apparatus. At its present stage of evolution the Madre research radar is a unique tool for investigating ionospheric perturbation phenomena of all types, with emphasis upon spectrum analysis as a principal analytical technique. For the purposes of this report, it is important that its characteristics as a coherent-pulse-doppler radar be understood; hence a short description of these characteristics follows:

(S) In its earlier configuration, when the studies to be reported here were begun, the Madre signal processor relied upon a rotating magnetic drum for storage of up to 420 seconds of range-gated signal data in an undetected video format. These data were made available to a scanning doppler filter which provided doppler resolution of about 1 Hz in the configuration used for this study, although the resolution could be changed by changing scanning filter bandwidths. The principal point here is that coherent bandwidth narrowing of signal information was employed to yield a 1-Hz-resolution bandwidth display of data from a selected range bin for a period as long as 420 seconds. For the data described in this report a 180-second storage period was used, along with an effective range-gate width of 670 μsec. The data were displayed as doppler shift vs time.

(S) Because this report is involved with propagation, it is important that the antenna used in this study be described. The antenna is the elevated one at the right in Fig. 1, photographed from the north. The center of this antenna is 205 feet above the cleared surface, within gently rolling forested land, which forms the reflecting surface at most azimuthal positions, including the direction of the Eastern Test Range at Cape Kennedy, and is 315 feet above the surface of the Chesapeake Bay, which forms the reflecting surface for easterly propagation. The antenna consists of a pair of horizontal dipole elements in a 90-by-70-foot-aperture corner reflector, and it may be positioned to any azimuth. To the left and below the rotatable antenna in Fig. 1 is a broadside array used for studies of over-the-horizon aircraft and radar and radio astronomy experiments. Figure 2 is a measured elevation-plane pattern for the rotatable antenna near midband,

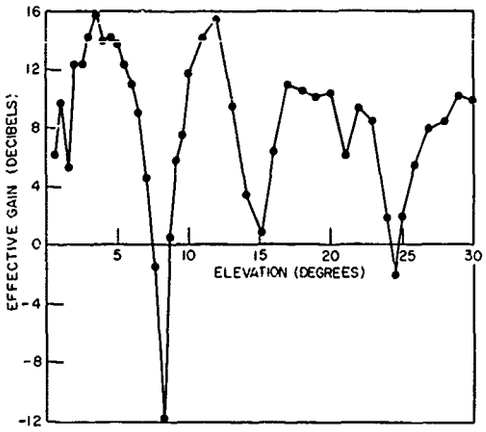

Fig. 2 - Measured elevation-plane pattern of rotatable antenna at 15.6 MHz, with the antenna oriented in southerly direction (U)

showing the excellent coverage at this frequency in the 2 to 7 degree elevation region which is important for F-layer transmission to the Eastern Test Range. This pattern, as well as similar data at two frequencies near the lower and upper extremes of the Madre radar's operating bandwidth, was acquired with a specially instrumented KC-135 aircraft from Rome Air Development Center, which flew a series of pattern flights for NRL in spring, 1966. These data have been important factors in the ionospheric ray-tracing program utilized in the signature analysis presented below.

(S) An additional feature of the Madre research radar which permits its high sensitivity is the provision for removal of the overwhelmingly large ground clutter (or ground-backscatter) return which seriously impairs the effectiveness of noncoherent ionospheric radars. A series of crystal comb rejection filters attenuates by 70 to 80 dB the large clutter signal (whose spectrum is normally concentrated within 1 or 2 Hz of the center frequency and prf-associated harmonics) without degrading moving-target echoes whose doppler-shifts do not fall within the rejection notches.

(S) Following is a list of the important parameters of the Madre research radar as it has been used in studies of ballistic missile launches from the Eastern Test Range:

Frequency band,	13.5 to 27.0 MHz,
Average power,	100 kW,
Peak power,	4.6 MW,
Antenna gain (including estimated 5-dB imperfect ground enhancement),	15 to 20 dB,
Pulse length (at -20-dB points),	250 to 950 μsec,
Pulse repetition frequencies,	45, 60, 90, and 180 pps,
Automatic on-line coherent integration: Storage time,	10 to 420 sec,
Predetection filter bandwidths,	1, 1/3, or 1/10 Hz.

Purpose of the Ray-Tracing Study (U)

(S) The overall objective of the series of related investigations described in this report is to apply diagnostic ionospheric propagation techniques such as computer-assisted ray tracing to the understanding of ionospheric phenomena as manifested upon over-the-horizon radar. In the present stage of these investigations a digital-computer ray-tracing program has been developed which enables the user to perform analyses of the radar signal data due to moving targets at single-hop range from the radar site. This program has been used for the purposes of this report to analyze radar data from several submarine-launched Polaris A2 and A3 ballistic missiles launched on the Eastern Test Range from Cape Kennedy.

(S) The coherent-pulse-doppler feature of the radar signal processor permits a direct measurement of vehicle doppler shift, or velocity, and the spectral dispersion of the radar signal permits an analysis to be made of the character of the target as a reflector, combined with the effects of turbulence in the intervening medium. The use of ionospheric soundings from points along the radar propagation path allows a model of electron density to be constructed from which propagation paths (or rays) may be calculated between the radar and two regions of interest: the region of the earth from which ground-backscatter emanates and the position of the vehicle moving along its trajectory. This ray trace may be used in conjunction with measured ground-backscatter to refine the model of ionospheric electron density that was constructed. With these preliminary "controls" achieved, the simulated propagation path may be used with radar data from the vehicle itself to carry out an analysis of the target signature. It is hoped that, ultimately, this technique will be developed to a degree where the variation of a target's echoing cross section and the behavior of its echo spectrum can be used to deduce the effects of the vehicle upon its environment from their manifestations upon ionospheric radar signals.

(S) It is proposed also to apply these ray-tracing analysis techniques in determining the extent to which ground-backscatter information may be used as a diagnostic device for assessment of over-the-horizon radar target area illumination.

The Ray-Tracing Program (U)

(S) A detailed description of the digital-computer ray-tracing program and a subroutine which uses this program for the synthesis of ground-backscatter profiles appear in Ref. 1. The program is constructed to make use of vertical ionospheric soundings, or of true-height profiles which may be determined from soundings, to synthesize a spherically symmetric ionospheric layer structure. Rays are calculated on the basis of a simple Snell's law treatment in a spherically stratified medium of varying index of refraction, exclusive of the effects of the geomagnetic field. The stratification is at present arbitrarily constrained to yield strata at a constant thickness of 1 km, except that for regions where electron density changes rapidly with height a provision is included for permitting a variable stratum thickness in order to increase the precision of the refraction treatment. Simple reflection of each ray about a vertical axis through path midpoint is assumed for the downward portion of its trajectory. Rays may be calculated for any elevation separation, although a separation of 0.05 to 0.1 degree is chosen for most calculations. To aid in calculating path absorption, ground and target illumination, and received signal amplitude from both earth backscatter and other targets, antenna parameters in azimuth and elevation are inserted into the program. For earth backscatter calculations an integration is performed over the azimuthal pattern, whereas for small-target echo amplitude calculations antenna gain only in the target direction is considered. For display purposes, the spacing of ray trajectory lines is weighted on the ray plot in

inverse proportion to the power density radiated in the appropriate direction by the antenna. For cases in which ground backscatter alone is treated, this display represents a vertical cut of the propagation geometry taken in the plane of the antenna beam center. For cases in which a missile launch is treated (into which class all of the examples in this report fall) the display represents a collapsed ensemble, presented in a single plane, of ray paths computed in a fan-shaped series of vertical planes which each contain the radar site and the missile position at a different point along its trajectory. Figure 3 is a perspective drawing of three such planes of radar site and missile position. The three ray trajectories in Fig. 3 would appear undistorted on a ray plot at their appropriate elevation positions, and the points P_1, P_2, P_3 would be joined on this presentation in a much-distorted facsimile of the missile trajectory that would be faithful only in showing the correct vehicle position along each ray path.

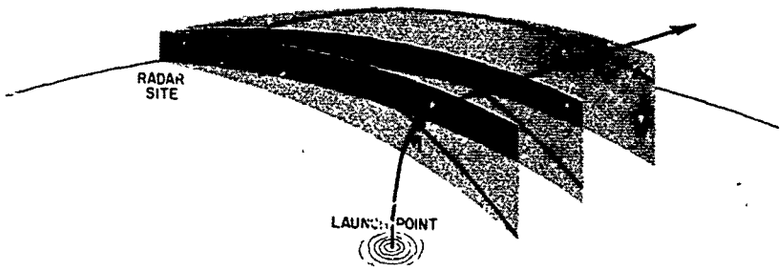

Fig. 3 - Perspective view of three adjacent vertical planes upon which ray trajectories are shown emanating from the radar site and intersecting the missile trajectory (U)

(U) In calculating the ground-backscatter amplitude expected from a selected ionospheric model a full set of ray trajectories is calculated from the radar site to the illuminated region of the earth at one-hop distance. Path absorption is calculated on the basis of an empirical formula determined by Lucas and Haydon (2). In the scattering model used the proportion of power available for diffuse scattering is determined arbitrarily (and a provision is made for an iterative procedure by which this proportion may be adjusted to fit the actual amplitude of the received ground-backscatter echo). A dependence of diffuse scattering amplitude versus elevation angle also is assumed (with a provision for subsequent adjustment to fit the measured ground-backscatter variation in time delay). Rays then are repropagated from incremental areas of the illuminated region, using the same propagation geometry from each area as was used for the initial ray trace to the illuminated region, and the contributions along all possible paths to the radar site from all incremental areas in the illuminated region are summed and displayed as amplitude versus path time delay. Examples of this presentation will be presented in comparison with received ground-backscatter signals in the Data and Analysis section.

(S) The propagation analysis also is used to determine predicted doppler shift and range to the position of a target with a known trajectory in the region illuminated. Doppler shift is calculated on the basis of rate of change of phase path and is presented versus time after launch in a graphical display. Examples of this presentation will be presented in comparison with actual radar data in a similar format in the Data and Analysis section.

Objective of This Report (U)

(S) This report contains analyses of several Polaris A2 and A3 launches on the Eastern Test Range from application of the techniques described. The principal effort in these analyses has been to determine the efficacy of the ionospheric propagation simulation in predicting:

- Illumination of the single-hop region from which the launches took place,
- Onset and loss time of target signature,
- Doppler shift of target echoes, and
- Intermittency of target echoes as caused by antenna parameters and propagation constraints.

(S) It should be borne in mind that these analyses are not presented as an exhaustive treatment of Polaris missile signature characteristics. They represent the results of one stage of a continuously evolving program in ionospheric propagation analysis and should be expected to be augmented by additional information and to be refined themselves as this program continues to develop. A thorough treatment of ten Polaris missiles by the techniques described appears in Ref. 1. This earlier work has been directed at using unrefined ionospheric sounding data to synthesize earth backscatter profiles for comparison with actual observed data and also to synthesize missile signature data for comparison with observed signatures. It has been found that ionospheric soundings alone could be used with substantial success in both endeavors and in fact that many characteristics of the earth backscatter echo and missile signature for a particular illumination situation and corresponding missile launch could be predicted with remarkable regularity. The following is a list of the successes of this "first-iteration" ray-tracing and earth backscatter simulation process:

Prediction Successes of Ref. 1 for Earth Backscatter Characteristics (U)

- Location and extent of regions of the earth illuminated.
- Location and relative intensity of localized illumination peaks within these regions.
- Positions of illumination nulls and their attribution to either ionospheric layer structure or antenna pattern effects.

Prediction Successes of Ref. 1 for Missile Signature Characteristics (S)

- Onset and loss times.
- Doppler shift.
- Temporary losses due to illumination voids.

Certain consistent failures of the technique involved cases in which local ionospheric layer pecularities, such as sporadic-E, made the spherically symmetric ionospheric approximation invalid. Their effects normally have degraded the precision of signature onset and early signature doppler shift predictions.

(S) The particular purpose of this report is to describe a second-iteration procedure which has been begun in an attempt to refine the ionospheric sounding data and match predicted earth backscatter distribution to actually observed data. In general, the procedure which has been followed begins with the first-step earth backscatter synthesis treated in Ref. 1 and described briefly above. Positions of predicted local peaks within the illuminated region are compared with observed data. Such localized peaks can be attributed in part to layer focusing effects and in part to the radiation pattern of the antenna. The focusing effects manifest themselves in stationary points on curves of time delay versus elevation takeoff angle, that is, points where time delay remains constant over a finite increment of elevation. These time-delay-focusing peaks may be associated, in a parametric sense, with the slope of an ionospheric electron-density versus altitude plot. Thus they may be intensified or attenuated, and moved about in time delay, by manipulating the slope of an ionospheric true-height profile; hence they may be in effect matched to observed profiles of earth backscatter versus time delay. The second iteration implied by this technique has been applied to three of the earth backscatter and Polaris missile signature cases treated in Ref. 1. Because the procedure followed is devoted to exploring the possibilities of this technique, some freedom has been exercised in manipulating the ionospheric density profiles. The major constraints which have been obeyed have been the purely subjective ones of (a) refraining from changing the profiles in any way which makes them inconsistent with normal ionospheric structure, (b) attempting to change profiles at appropriate positions to conform to the true indicated layer structure, and (c) avoiding wholesale changes which would result in large alterations in the structure of the simulated ionosphere at any height. In addition, it has been attempted where possible to constrain changes so that the resultant simulated profiles are bounded by the extremes indicated by measured profiles from sounding stations along the propagation path.

DATA AND ANALYSIS (U)

(S) The pertinent launch and radar data for Eastern Test Range (ETR) launch 0303, of January 26, 1964, which is the first example treated, are as follows:

Missile type,	Polaris A2,
Launch time,	1459:06 EST,
Radar frequency,	13.56 MHz,
PRF,	90 pps,
Pulse length (-20-dB points),	700 μsec,
Average power,	100 kW,
Illumination mode,	E and F layers.

Figure 4 is a photograph of the earth echo acquired with the Madre radar. This illustration is a display of received echo amplitude versus time delay, and was photographed at the first receiver intermediate frequency (500 kHz) stage with no bandwidth-narrowing or detection. A time exposure of several seconds was made to smooth out the typical 2- to 3-sec fading period of earth backscatter and hence to eliminate as nearly as possible the sampling effect of this type of presentation. A sequence of calibration pulses at approximately 1 mV peak-to-peak amplitude appears on this photograph, with a spacing of approximately 5.5 msec. It is apparent from Fig. 4 that the earth backscatter echo begins as close as 6 msec and extends approximately to 16 msec in time delay, with peaks in amplitude at about 10 and 12 msec.

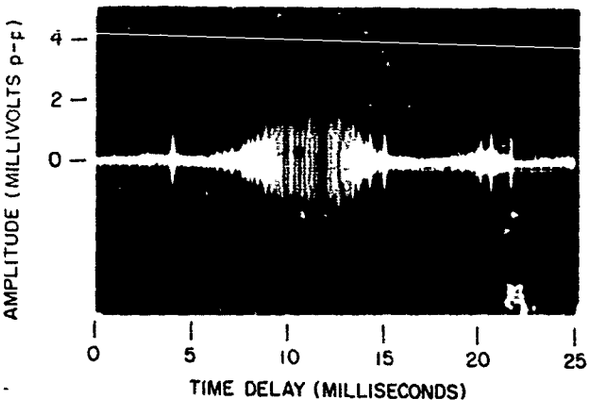

Fig. 4 - Observed ground backscatter distribution (near launch time), Jan. 26, 1964, ETR launch 0303 (S)

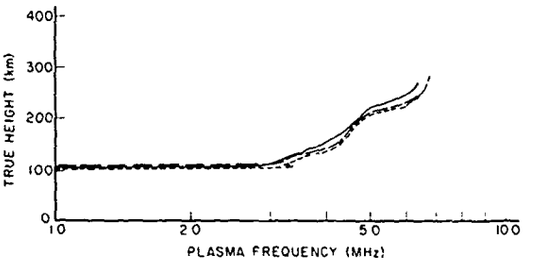

Fig. 5 - Ionospheric true-height profiles used in the first step (short-dashed curve), second step (long-dashed curve), and third step (solid curve) of the backscatter-matching procedure, ETR launch 0303 (S)

(U) Figure 5 is a collection of three ionospheric true height profiles, which represent different stages in the performance of the earth-backscatter matching procedure and are included here to demonstrate in detail the technique used. The short-dashed curve in Fig. 5 is a direct tracing of an ionogram from Grand Bahama Island, which was used for the first step of this analysis. The long-dashed curve and solid curve represent the second and third steps, respectively, in the process. Figure 5 illustrates the small (5 to 10 km) changes in height of the entire profile which were necessary to make the simulated backscatter match the leading edge of the observed echo. The various rates of curvature and critical frequencies of the F1- and F2-layer contributions illustrate the slope alterations which were introduced to move the amplitude peaks about in time delay and thus match the observed peak and null positions.

(U) Figure 6 is a collection of graphs showing the variation in time-delay behavior of the earth backscatter distribution which was accomplished by the ionospheric profile changes. Time-delay focusing occurs at the maxima and mimima of these curves, that is, at points where a significant change in the elevation takeoff angle corresponds to no significant change in the time delay. The progression from the short-dashed curve, corresponding to the Grand Bahama Island ionogram, to the solid curve, which represents the third step in the process, is apparent. The short-dashed curve, which continues below the horizontal axis to a sharp point and hence contributes no substantial focusing effect, is blunted to form an E-layer-focusing peak at 10 to 11 msec. The initial F-layer-focusing peak at 9 msec (indicated by the valley at 12 degrees elevation in Fig. 6) is drawn out to 12 msec to contribute the largest peak in the earth backscatter profile, while

the high-angle F-layer peak is drawn out to make a contribution at 12 msec also. The short notch at 13.5 msec time delay is a consequence of an attempt to add energy along the declining tail of Fig. 4, which extends from 12 to 15 or 16 msec. This notch does contribute a slight focusing peak.

(U) Figure 7 is a collection of the simulated earth backscatter profiles which resulted from these three steps, with the solid curve representing the third step. The emergence of large peaks near 10 and 12 msec is evident, as is an enhancement of the echo between 12 and 16 msec time delay.

(U) Figure 8 contains tracings of true-height profiles from Grand Bahama Island (GB) and Cape Kennedy (CK), together with the simulated ionospheric true height profile which resulted from a fourth, and final, step of the iteration. The existence of the localized, blanketing E layer at Cape Kennedy shown in Fig. 8 is not apparent in the observed earth backscatter data, which can be seen from the dashed curve in Fig. 8 to be best synthesized by an ionosphere similar to that measured at GB, but slightly raised.

(U) Figure 9 contains graphs of the ionospheric earth backscatter profile which resulted from the final step of the iteration plus (transcribed from Fig. 4) a short-dashed curve sketched in to indicate the envelope of the observed earth backscatter echo for comparison. The long-dashed and solid curves illustrate the effect of introducing into the ray tracing procedure the antenna elevation plane radiation pattern. The long-dashed curve represents the earth backscatter profile to be expected from an isotropic radiator provided with enough power to equal the radiation density at the lobe peak of the true, ground-dependent radiator, whose effects are represented by the solid curve. Antenna pattern effects sharpen the leading edge of the echo and deepen the nulls at 11 and 14.5 msec time delay. The final version of the simulated earth backscatter echo matches the observed one in the position of the major peak (within 0.3 msec), two of the secondary peaks (within 0.5 msec), and in general appearance. A further step in the iteration could possibly draw the leading edge inward to match the first observed peak and might permit an additional peak to be inserted in an intermediate position. It is believed, however, that the remaining discrepancy between the observed and simulated versions in Fig. 9 arises from a geographical asymmetry in the ionosphere. The GB and CK ionograms in Fig. 8 illustrate that the E layer, to which this remaining discrepancy may be ascribed, displays a marked geographical variation.

(S) Figure 10 is a plot of the ray profile which was obtained from the final version of the simulated ionosphere for ETR launch 0303. As mentioned, the ray density in elevation is proportional to the radiated power in the indicated directions, permitting a graphical representation of the antenna radiation pattern. It should be noted that the height scale of Fig. 10 and of other ray plots that will follow is expanded by a factor of two relative to the range scale. This expedient was introduced to permit closely spaced rays to be discerned. The missile trajectory is indicated by the curved line rising from a range of 1170 km, the position of the Eastern Test Range. Both E- and F-layer contributions are evident at all ranges in Fig. 10; the former contributes the earliest missile trajectory illumination, and the latter continues the illumination to an altitude of about 165 km, with very low amplitude illumination up to 185 km. The void in the ray pattern at 120 to 150 km altitude and slightly closer in range than the missile trajectory is a common phenomenon caused by a combination of an antenna pattern null and E-layer cutoff. Under some conditions, this type of void can fall on a missile trajectory and will then give rise to a temporary signature loss.

(S) Figure 11 is the simulated signature of ETR launch 0303 showing a predicted signal onset at 35 seconds after launch, and continuous reception from that time until more than 150 seconds after launch. This illustration is composed so that all data fall

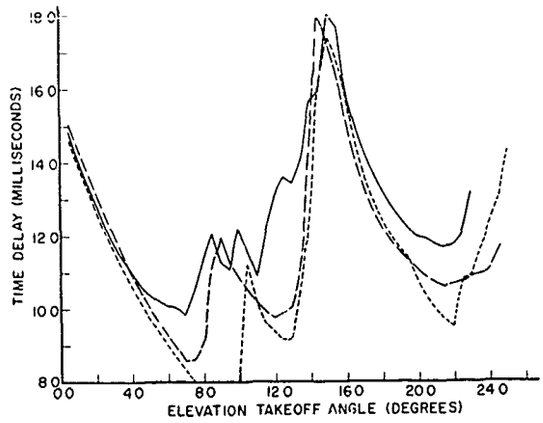

Fig. 6 - Path time delay versus radiation takeoff angle for the first (short-dashed curve), second (long-dashed curve), and third (solid curve) steps of the backscatter-matching procedure, ETR launch 0303 (S)

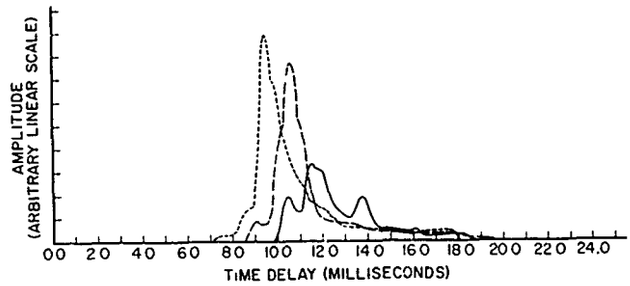

Fig. 7 - Earth backscatter versus time delay for three steps of the backscatter matching procedure, ETR launch 0303(S)

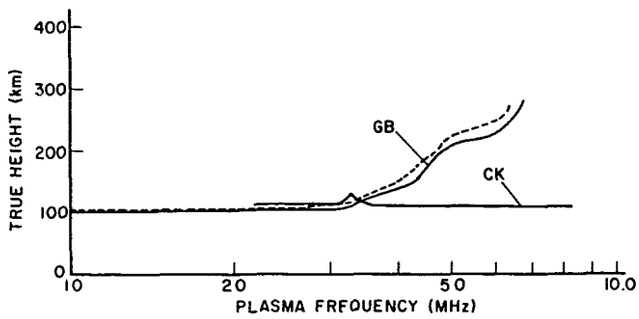

Fig. 8 - Ionospheric true-height profiles from Grand Bahama Island (GB) and Cape Kennedy (CK), together with the final, fourth-step, backscatter-matched version, ETR launch 0303 (S)

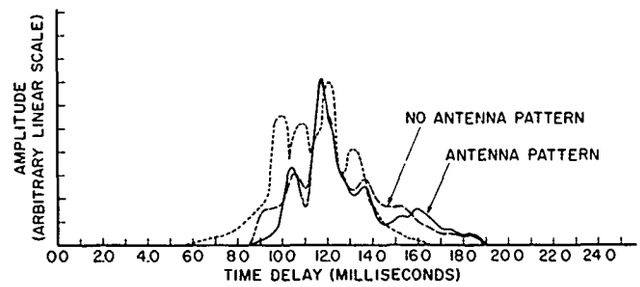

Fig. 9 - Earth backscatter versus time delay for the final, backscatter-matched ionospheric profile compared with observed data, ETR launch 0303 (S)

Fig. 10 - Ionospheric ray plot for ETR launch 0303 indicated by the curved line (S)

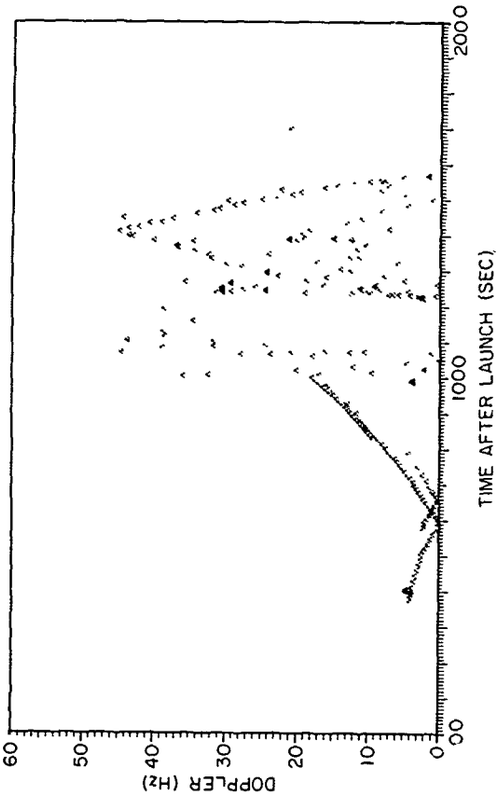

Fig. 11 - Simulated signature for ETR launch 0303 (S)

into the 0 to 45 Hz doppler-shift band. The Madre radar, like all pulse-doppler devices, is limited in unambiguous doppler sensitivity by its pulse-repetition frequency (prf). For the 90 pulse-per-second (pps) rate which was used during this launch the available unambiguous doppler interval extends from 0 to 45 Hz; all data below zero (i.e., all negative doppler shifts, or receding targets) are "reflected" into this interval, as are all data for the several contiguous 45-Hz intervals through which an accelerating missile's doppler shift passes. A multiplicity of paths is seen to contribute to the signature in Fig. 11 during much of its duration. Figure 12 is the observed version of the missile signature, with superimposed upon it a line corresponding to the simulated signature from Fig. 11. The changes of the line between white and black are of no significance other than to enhance its visibility. There is in Fig. 12 a likely error in the doppler-shift scale of the observed signature. A high-pass filter in the signal processor normally limits the data displayed to a band between 5 and 45 Hz, but in this case traces appear as low as 2.5 Hz, and it may be surmised that the entire display should be raised by 2.5 Hz relative to the scale baseline. Finally, there appear on Fig. 12 a number of short horizontal traces between 8 and 30 Hz which are simply manifestations of an interfering radio signal and should be ignored. This interference must be recognized as a contaminant of the data, however, whose chief effect here was probably to lower overall radar sensitivity. In all likelihood the absence of missile signature data after the first, intense E-layer contribution (20 to 105 sec after launch) is partially a symptom of this degraded sensitivity. The simulated and measured signatures may be seen to match extremely well from the observed onset time of 20 sec after launch until loss of the signal at about 105 sec after launch. Absence of the signal after this time, neglecting for the moment the degraded system sensitivity due to interference, indicates that the F-layer illumination actually achieved may have been a great deal less intense than predicted, a situation which could stem from more intense E-layer blanketing than was predicted. The pronounced, early signature displayed in Fig. 12 suggests that the possibility of E-layer blanketing is, indeed, a strong one.

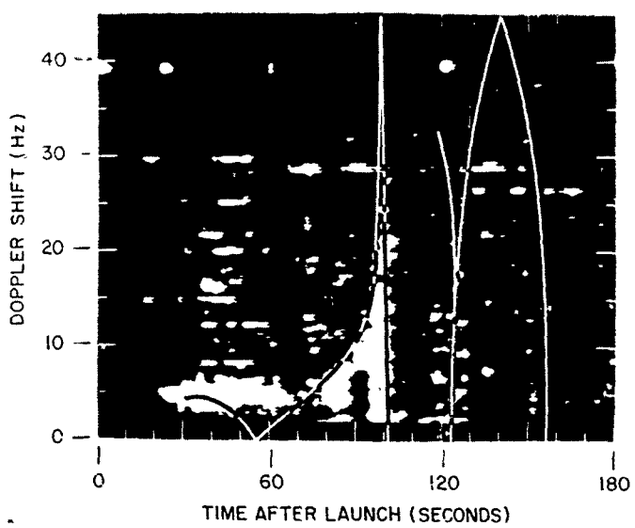

Fig. 12 - Observed signature for ETR launch 0303, with backscatter-matched simulation from Fig. 11(S)

(S) The improvement in earth backscatter simulation and in signature prediction which has been accomplished by the backscatter matching procedure can be seen by comparison with the results of the one-step prediction method described in Ref. 1. Figure 13 is a predicted earth backscatter profile acquired by using unmodified ionosonde data from GB, together with a representation (dashed curve) of the observed earth backscatter profile. The improvement in several aspects of the backscatter simulation of Fig. 9, the resultant of the backscatter-matching procedure, is evident. (Note that Figs. 9 and 13 are to slightly different horizontal scales.) The simulated backscatter curve in Fig. 9 (with the antenna pattern included) matches the rising and falling portions of the measured version (short-dashed curve in each figure) much more accurately than does the predicted curve in Fig. 13. In addition, the large, central peak in the former is much closer in time delay to that actually observed than in the latter. This improvement manifests itself slightly in the predicted missile signature for this case. Figure 14 contains a simulated signature from the single-step prediction method superimposed on the same observed signature as appears in Fig. 12. It is clear from comparison of the simulated signature in Fig. 14 with that in Fig. 12 that the latter is more faithful to the measured data along the rising-doppler portion of the curve, from 55 to 100 sec, in the rapid decline which terminates at 102 sec, and in the loss of signal which occurs there. The simulated signature in Fig. 12 does predict reappearance of the signature at 120 sec, an event which does not occur, but degraded system sensitivity or a blanketing E layer could be at fault.

(S) Eastern Test Range launch 2955, of May 25, 1964, is a second example of the application of this backscatter-matching procedure to a missile-launch signature. The important launch and radar data for this operation are as follows:

Missile type,	Polaris A3,
Launch time,	1415:03 EST,
Radar frequency,	15.595 MHz,
PRF,	90 pps,
Pulse length (at -20-dB points),	700 μsec,
Average power,	100 kW,
Illumination modes,	E and F layers.

Figure 15 contains tracings of the ionospheric true-height profiles (solid lines) determined from ionograms taken at Grand Bahama Island (GB) and San Salvador (SS) near the time of of launch, together with the final version (dashed) of the backscatter matching procedure. In this case it may be seen that the latter falls neatly into place between the two observed curves. Figure 16 contains a curve of simulated earth backscatter amplitude versus time delay for the backscatter-matched ionosphere, together with a dashed curve marking the observed earth-backscatter data. It is evident that the beginning and end of each of the two distributions, plus the number and placement of the largest local illumination peaks, are matched quite well. The relative amplitudes of the peaks are not well simulated, however.

(S) Figure 17 is the ray plot determined from the simulated ionosphere, showing in this case no substantial void in illumination coverage of the missile trajectory, but a good deal of ray focusing at several elevation angle positions. These focused bundles of rays are, of course, associated with the multiple-peaked earth backscatter distribution in Fig. 14. Termination of the missile trajectory in the midst of the ray plot occurs simply because range tracking data ended at that point.

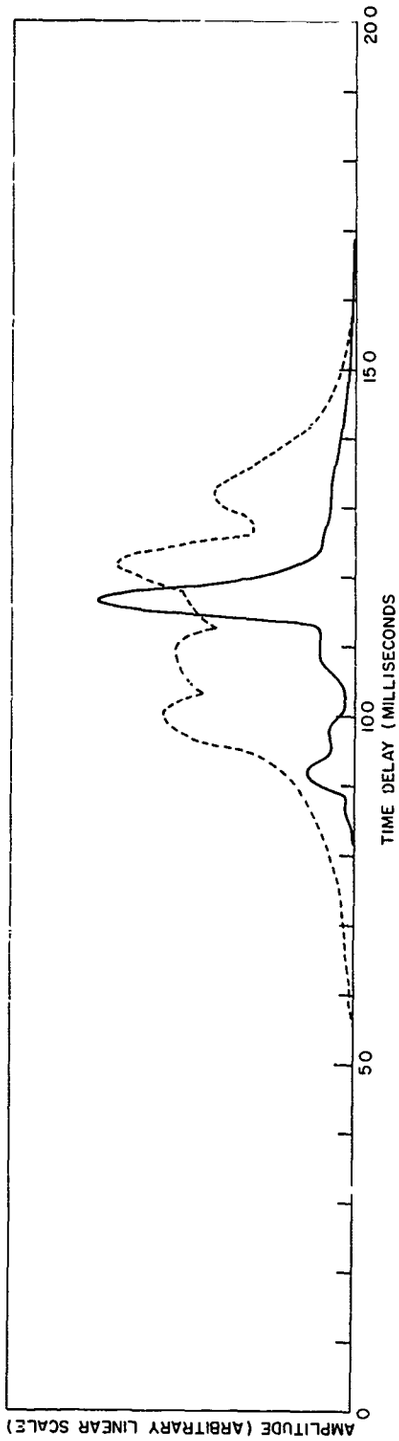

Fig. 13 - Curves of earth backscatter versus time delay for a raw, unmatched ionospheric profile (from Ref. 1) compared with observed data (dashed curve), ETR launch 0303 (S)

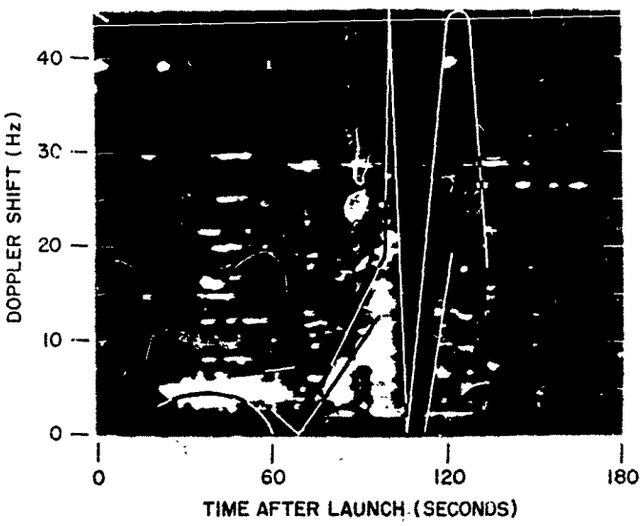

Fig. 14 - Observed signature for ETR launch 0303 compared with the unmatched simulation from Ref. 1 (S)

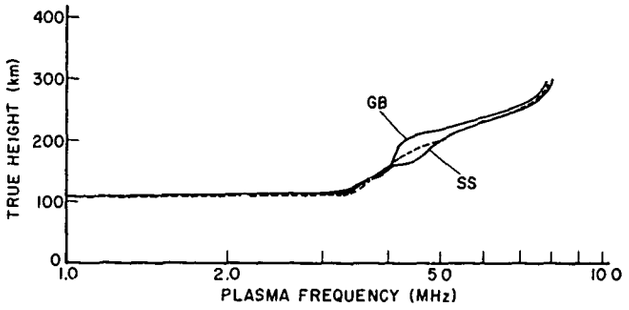

Fig. 15 - Ionospheric true-height profiles from Grand Bahama Island (GB) and San Salvador (SS) together with the final backscatter-matched version, ETR launch 2955 (S)

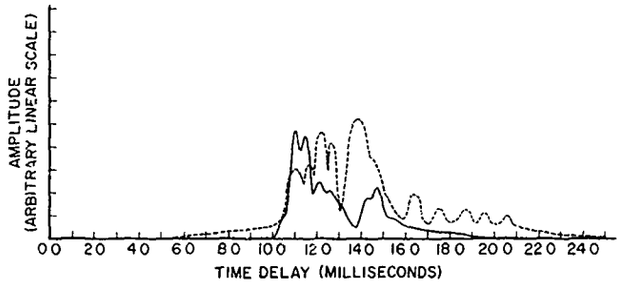

Fig. 16 - Earth backscatter versus time delay for the final ionospheric profile (solid curve) compared with observed data (dashed curve), ETR launch 2955 (S)

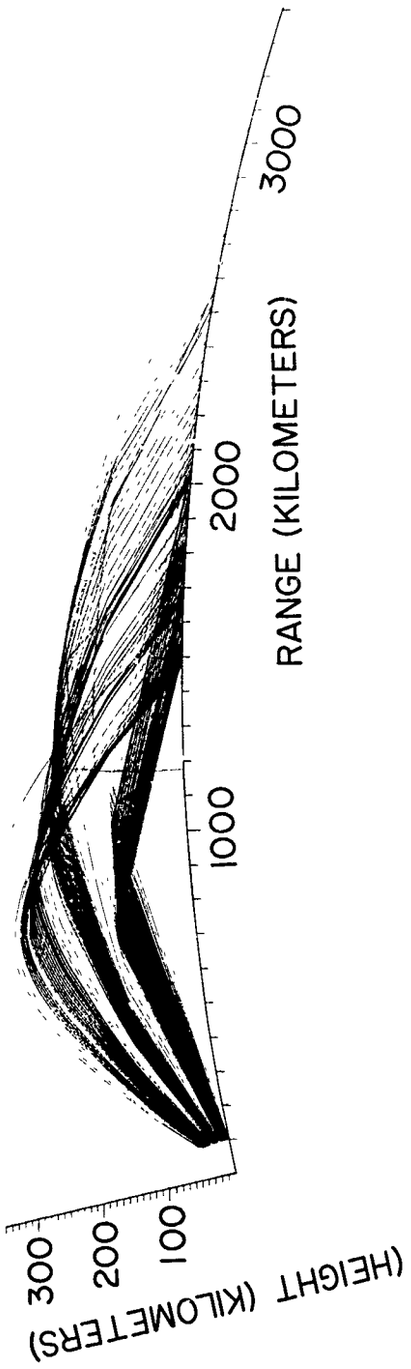

Fig. 17 - Ionospheric ray plot for ETR launch 2955 (S)

(S) Figure 18 is the simulated doppler-shift versus time display calculated with the aid of the ray trace. The discontinuous character of Fig. 18, particularly along the early portion of the trace, is due in this case to the sampled nature of the ray trace and to the limited accuracy of the computer operations. The latter portion of the signature, between 125 and 145 sec after launch, appears scattered in doppler shift because of multipath illumination, as may be seen on Fig. 17 to be prevalent above about 120 km.

(S) Figure 19 is a photograph of doppler shift versus time after launch measured with the Madre radar during the Polaris launch whose simulated signature appears in Fig. 18. The reader should be cautioned in interpreting this illustration that its format is not identical to that in Fig. 18, because the doppler-shift data are projected (or reflected) here not into the 0 to 45 Hz frequency interval, but into the -22.5 to +22.5 Hz frequency interval. For convenience in effecting a comparison between Figs. 18 and 19, the doppler-shift data from the former are overlaid on the latter in the appropriate format. Also included in Fig. 19, at a doppler shift of approximately +17 Hz, is a row of blobs at 0, 20, 60, 120, and 180 sec after launch. These blobs are simply timing marks.

(S) One final remark is pertinent to the circumstances of the comparison between the simulated doppler-versus-time behavior and the observed behavior in Fig. 19. The uncertainty in actual launch time (up to 1 sec possible error), plus whatever operator error may occur in the placement of the timing marks, all add to the effects of possible motions in the ionospheric reflection region (which would be undetectable to the radar) and combine to prevent precise placement of the simulated doppler-versus-time display upon the measured version. Approximately 3 sec leeway from the nominal launch time has been used in view of these uncertainties to permit a strikingly complementary orientation of the two plots. The signature onset at approximately 80 sec, its subsequent downward curvature and steep decline to -17.5 Hz, and the final downward trend of the observed signal at 130 to 140 sec, all agree with the simulated version. The brief absence of a signal between 120 and 130 sec, when the superimposed simulation rises from +5 to +22.5 Hz and back down to +7 Hz in Fig. 19, corresponds to the portion of Fig. 17 where the missile trajectory has just passed the initial (high-angle) bundle of focused F-layer rays and is traversing a region of low illumination density. The temporary loss of the observed signal thus is not inconsistent with the postulated ionospheric ray trace, and in fact represents a confirmation of the predicted illumination pattern. That the observed signature continues beyond the simulated one is of no significance, because the simulated signature ends when the range data end, and as may be seen in Fig. 17 this point falls amidst a strongly focused bunch of rays.

(S) Figure 20 is a plot of predicted earth backscatter from an unaltered ionospheric profile determined from GB ionosonde data, together with a representation (dashed curve) of observed data. It may be seen by comparison with the backscatter-matched version in Fig. 16 that the iteration procedure has resulted in a large improvement in the position of the leading edge of the predicted earth backscatter profile as well as in the number and distribution of local focusing peaks. Figure 21 is a simulated signature from the single-step prediction method superimposed on observed data. In this case, the improvement of Fig. 19 over Fig. 21 rests principally in the predicted signature onset time. In the former, onset is predicted at 60 sec, about 20 sec before the signal is actually received, but in the latter it is predicted an additional 22 sec earlier. Thus more than half of the onset time inaccuracy of the single-step signature prediction process has been eliminated. Although substantial differences between Figs. 19 and 21 also occur between 110 and 140 sec, there is no obvious indication of which is more faithful to the observed data.

(S) A third example of the computer simulation compared with actually measured ground backscatter and signature data of submarine-launched ballistic missiles is the

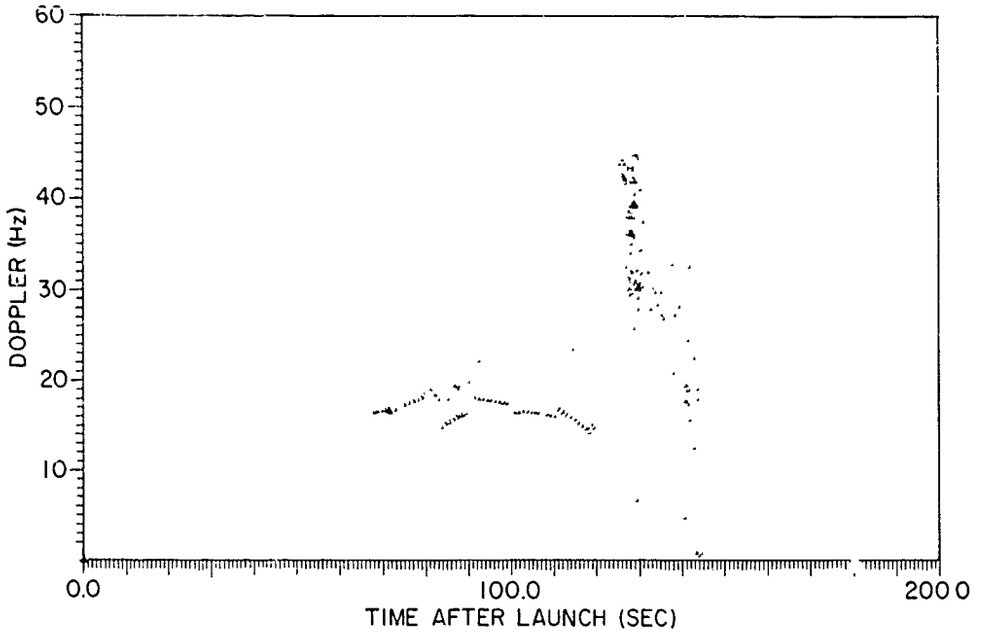

Fig. 18 - Simulated signature for ETR launch 2955 (S)

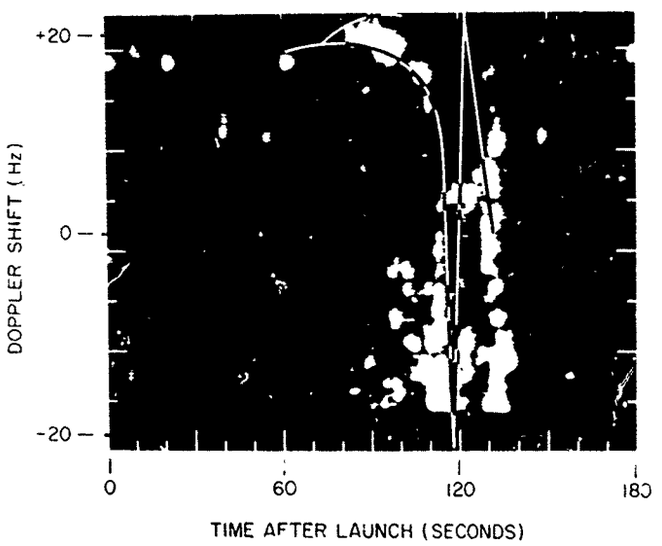

Fig. 19 - Observed signature for ETR launch 2955 compared with the backscatter-matched simulation of Fig. 18 (S)

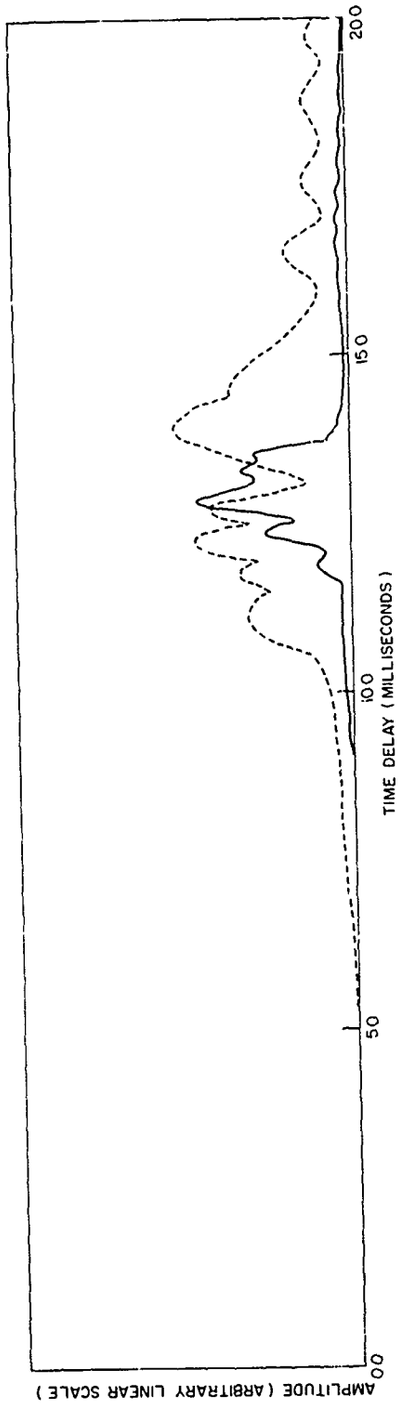

Fig. 20 - Earth backscatter versus time delay for raw, unmatched ionospheric profile (from Ref. 1) compared with observed data (dashed curve), ETR launch 2955 (S)

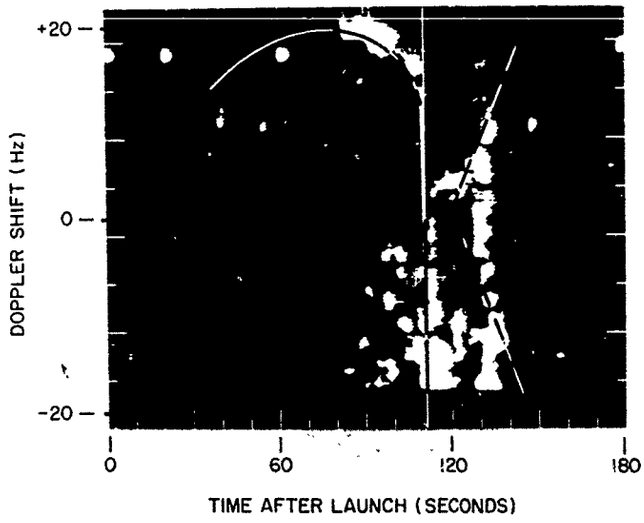

Fig. 21 - Observed signature for ETR launch 2955 compared with the unmatched simulation from Ref. 1 (S)

treatment of ETR launch 3670, of July 30, 1964. The pertinent launch and illumination data are as follows:

Missile type,	Polaris A3,
Launch time,	1130:03 EST,
Radar frequency,	18.036 MHz,
PRF,	90 pps,
Pulse length (at -20-dB points),	700 μsec,
Average power,	100 kW,
Illumination modes,	E and F layers.

(S) Figure 22 contains the usual tracings of ionosonde data, together with the final version of the backscatter-matched ionospheric true height profile. In this case, the best match to the F-layer earth backscatter contribution (the F-layer component was stressed over that from the E layer to illustrate the importance of the former in the late-time portion of the missile signature) arose from a simulated true height profile which fell between the measured ones. Figure 23 is the curve of simulated earth backscatter with superimposed upon it a dashed curve representing the observed data. The simulation is successful in predicting most aspects of the observed data beyond 12 msec, but does not properly treat the leading edge. The feature of Fig. 23 which is of most interest is that it does show agreement between the predicted and observed earth backscatter data at time delays between 12 and 20 msec; the interval from 16 to 18 msec, where a shallow null in coverage appears, can be seen on the ray trace of Fig. 24 (with a small amount of imagination) to represent a void in earth illumination between E- and F-layer coverage. That this layer cutoff effect leads to a concomitant void in illumination of the missile trajectory is also evident from Fig. 24.

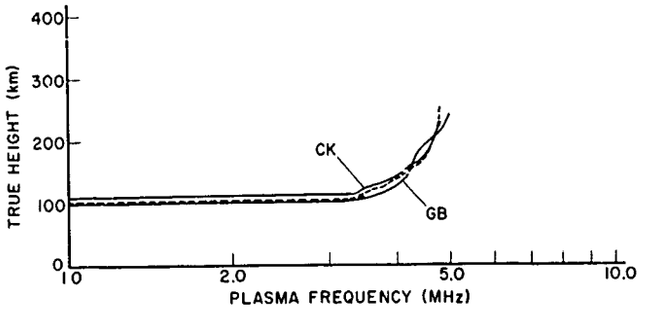

Fig. 22 - Ionospheric true-height profiles from Cape Kennedy (CK) and Grand Bahama Island(GB) together with the final F-layer backscatter-matched version, ETR launch 3670 (S)

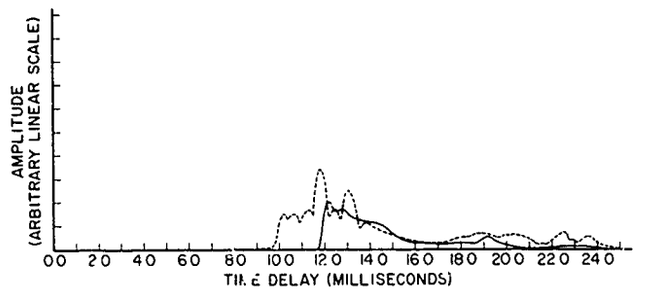

Fig. 23 - Earth backscatter versus time delay for the final, F-layer matched ionospheric profile compared with observed data (dashed curve) ETR launch 3670 (S)

(S) Figure 25 is the simulated version of the missile signature. The early part of this graph, from signature onset at about 90 sec until a temporary loss of signal at about 118 sec after launch, corresponds to E-layer illumination. The steeply sloped line between 122 sec and 136 sec after launch can be attributed to F-layer illumination.

(S) Figure 26 is the observed signature from ETR launch 3670, with superimposed upon it the simulated version. Agreement may be seen to exist in onset time (within about 15 sec) and in the detailed behavior of the E- and F-layer portions of the signature. The absence of a signal between 90 and 110 sec after launch is a somewhat exaggerated reflection of the E-layer cutoff illumination void predicted by the ray trace. Very close agreement between the simulated and observed signatures is also found in their ultimate loss at 135 to 140 sec, and it is this late-time signature behavior which has been the chief object of the simulation in this attempt.

(U) An effort has been made, in a second backscatter-matching process, to stress the leading edge portion of the earth backscatter, somewhat at the expense of the later time-delay, F-layer contribution, to more accurately predict the initial appearance of the missile signature. Figure 27 contains the ionosonde data, together with (dashed) the final version of the backscatter-matched ionospheric true height profile for this case. The dashed curve may be seen to be closer to the GB version than in Fig. 22, with a

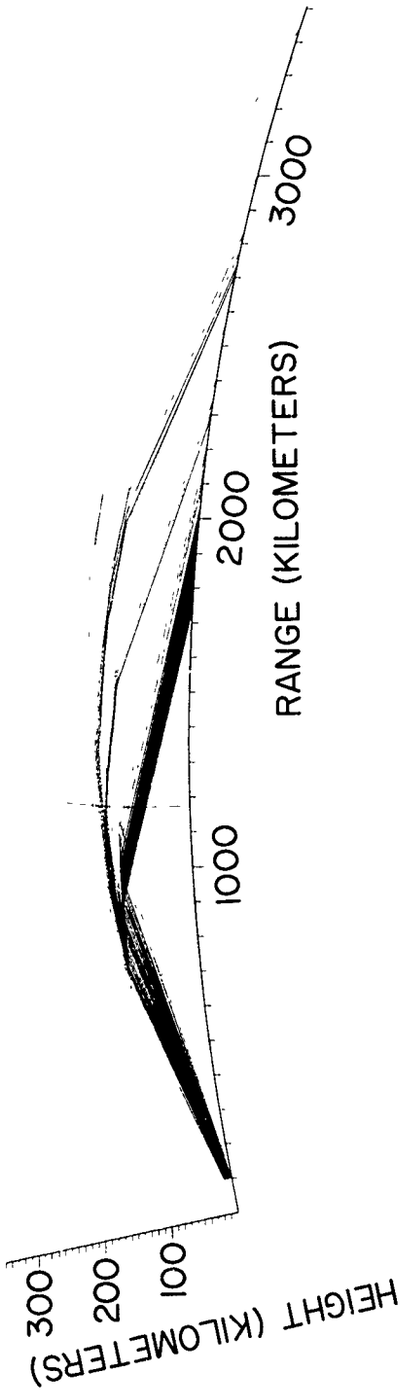

Fig. 24 - Ionospheric ray plot (F-layer matched) for ETR launch 3670 (S)

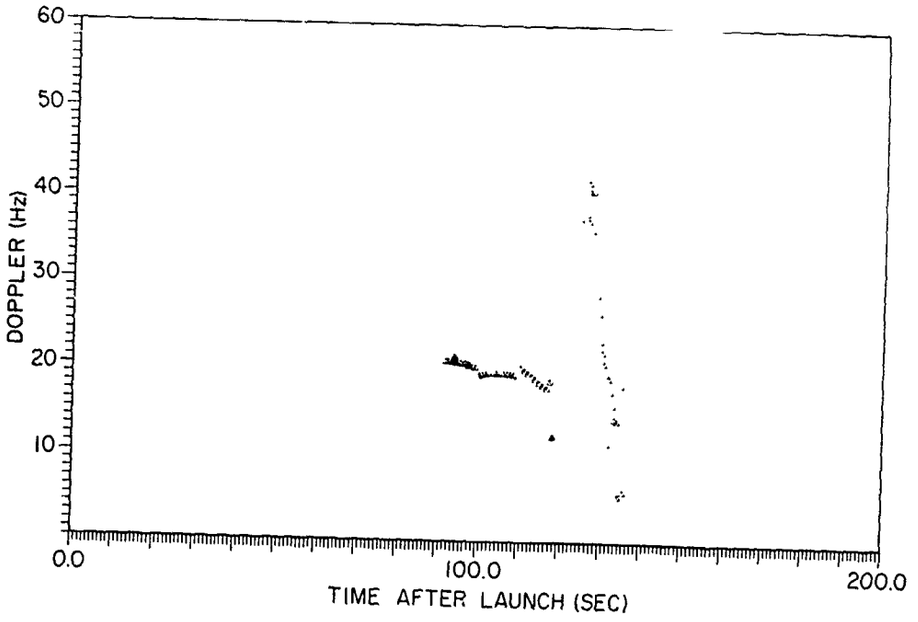

Fig. 25 - Simulated signature (F-layer matched) for ETR launch 3670 (S)

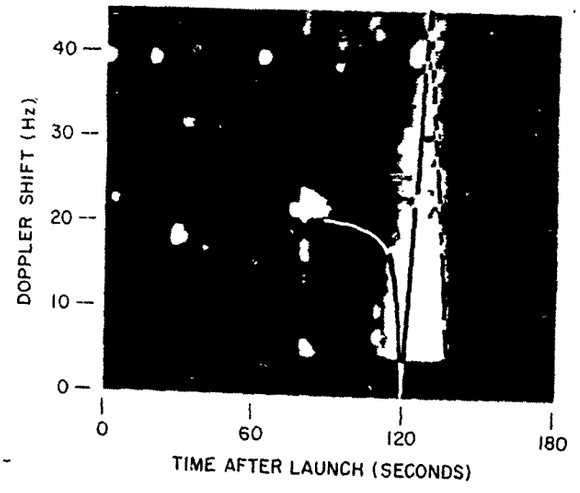

Fig. 26 - Observed signature for ETR launch 3670 compared with the (F-layer matched) simulation of Fig. 25 (S)

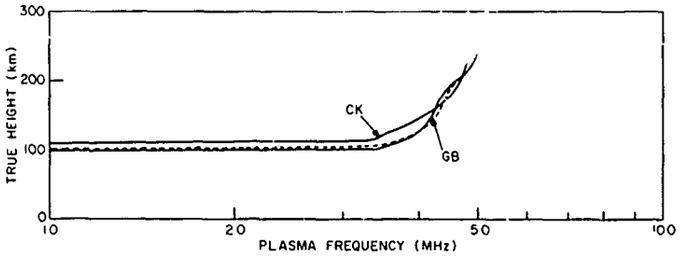

Fig. 27 - Ionospheric true-height profiles from Cape Kennedy (CK) and Grand Bahama Island (GB) together with the final, E-layer backscatter-matched version, ETR launch 3670 (S)

similar slight elevation but lesser alterations in curvature than in the earlier simulation. Figure 28 is the curve of simulated backscatter, with the dashed curve superimposed to represent observed data (a discrepancy exists in the amplitude scale between Figs. 28 and 23, but each is properly scaled relative to the observed data shown). Both the leading and trailing edges of the major earth backscatter contribution and the relative spacing of the two principal peaks are simulated to within 0.6 msec. The relative heights of these peaks is also predicted rather well. Figure 29 is the ray trace for this case, showing a good deal less F-layer illumination but somewhat more E-layer illumination than Fig. 24.

(S) Figure 30 is the simulated version of the missile signature, showing earlier acquisition and earlier loss than the simulated version in Fig. 25. Figure 31 is the observed signature once more, with the latest simulated version superimposed upon it. The agreement in onset time has been improved to within 5 sec, but an error has been introduced into the time of signal loss.

(S) This treatment of ETR launch 3670 has involved efforts to synthesize, in separate attempts, the earth backscatter which best matches the farther extreme of the path and the earth backscatter which best matches the closest portion of the path. Thus the profile in Fig. 23 fails to match the E-layer contribution fully, and that in Fig. 28 fails to match the later portion of F-layer coverage. Figure 32 contains a curve of earth backscatter versus time delay which was determined in Ref. 1 by treating E- and F-layer propagation separately and plotting the predicted backscatter profiles on the same axes. The large hump between 9 and 17 msec on Fig. 32 arises principally from E-layer illumination, and the smaller contribution between 19 and 24 msec arises from F-layer illumination. The dashed line represents measured data and at first glance suggests that the separate E- and F-layer treatments permit a superior match to observed data than the single profile manipulations which yielded the results shown in Figs. 23 and 28. However, the artificiality inherent in the former betrays itself when an attempt is made to predict a missile signature from the illumination simulated by this two-ionosphere superposition. Figure 33 displays the predicted signature appropriate to this dual ionosphere superimposed upon the observed signature. The E-layer contribution, shown as a solid line, begins at about 45 sec and continues until 120 sec after launch. The (dashed) F-layer contribution begins immediately thereafter, and continues until 135 sec. When this illustration is compared with the results of the backscatter-matched profile, shown in Figs. 26 and 31, the advantages of the procedure are evident. Not only does backscatter matching permit a much more precise determination of signal onset, but it yields a large improvement in doppler-shift measurement during the life of the signature. Indeed, the simulated signature in Fig. 26 departs from the observed one only in that it predicts onset about 15 sec later than was experienced. This failure can be attributed directly to

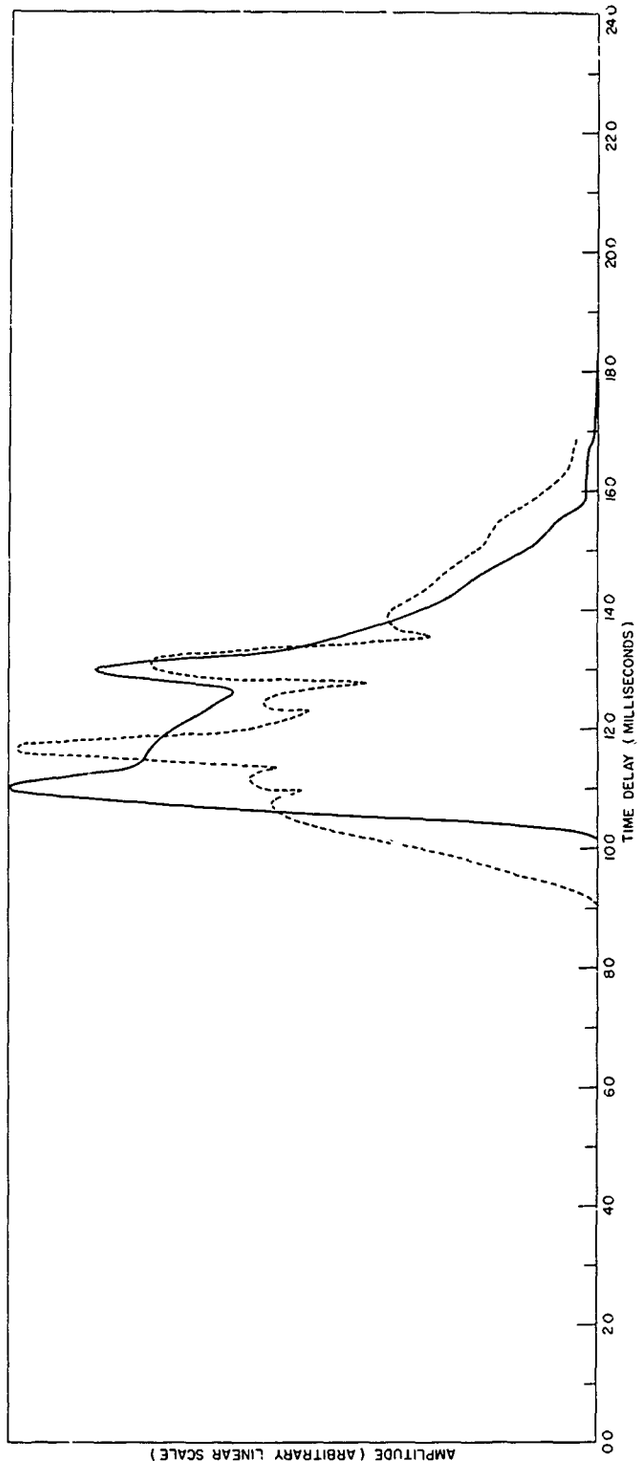

Fig. 28 - Curves of earth backscatter versus time delay for the final, E-layer matched ionospheric profile compared with observed data (dashed curve) ETR launch 3670, (S)

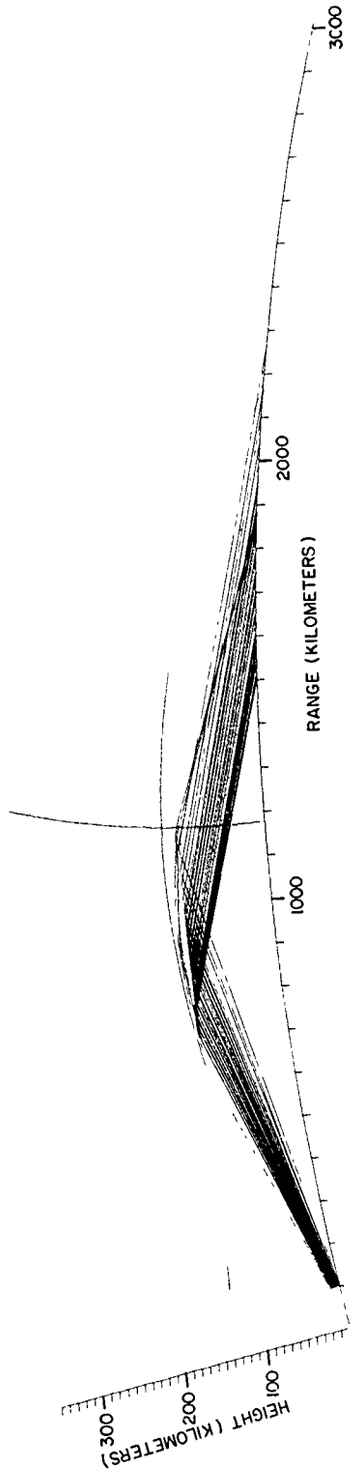

Fig. 29 - Ionospheric ray plot (E-layer matched) for ETR launch 3670 (S)

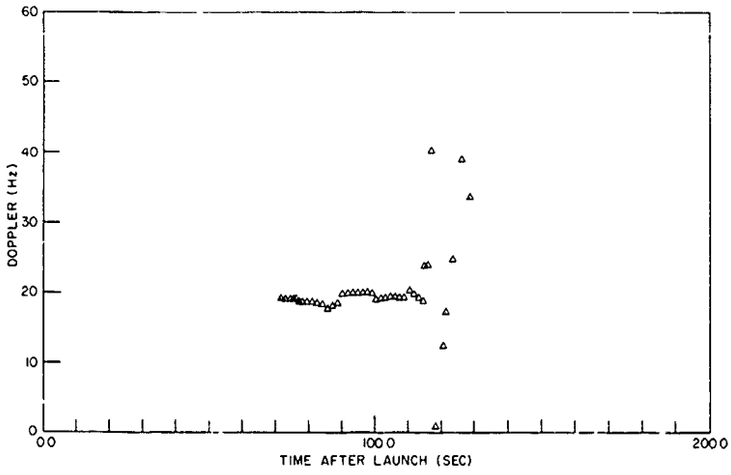

Fig. 30 - Simulated signature (E-layer matched) for ETR launch 3670 (S)

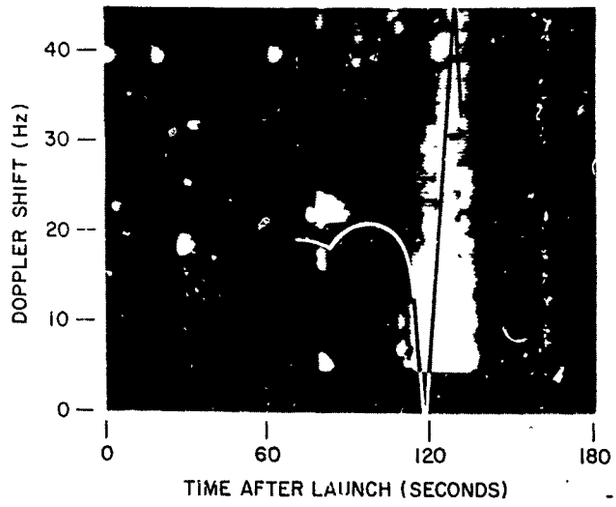

Fig. 31 - Observed signature for ETR launch 3670 compared with the E-layer matched simulation of Fig. 30 (S)

the near-range E-layer echo, which may have resulted from a patchy or semitransparent layer structure, and is not satisfactorily treated by the ray tracing process. It is of interest that closer attention to the leading edge of the earth-backscatter echo, resulting in the simulated signature in Fig. 31, improved the predicted time of onset by 10 sec.

(S) The introduction of an artificial E layer, as was attempted in Ref. 1 to yield the predicted backscatter profile of Fig. 32, has resulted in a gross error in prediction of signature onset. The attempt to use a single-backscatter-matched ionospheric profile

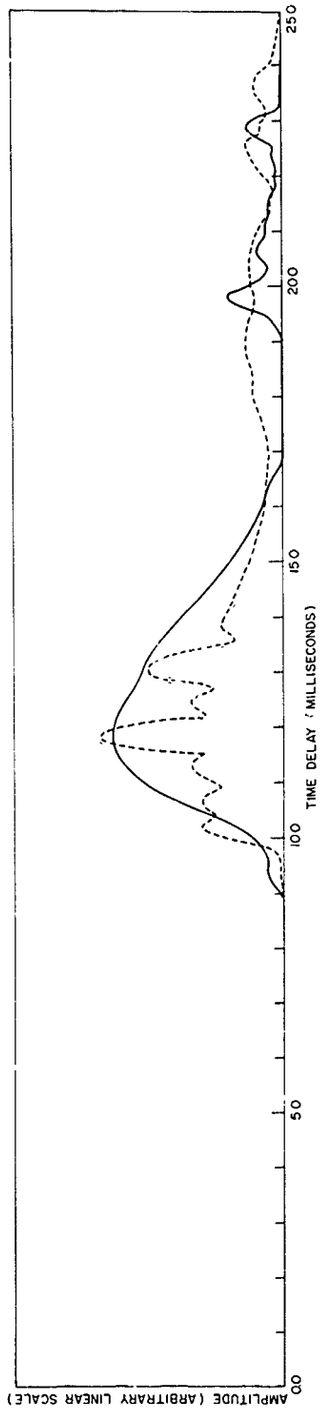

Fig. 32 - Earth backscatter versus time delay for raw, unmatched ionospheric profile (from Ref. 1) compared with observed data (dashed curve), ETR launch 3670 (S)

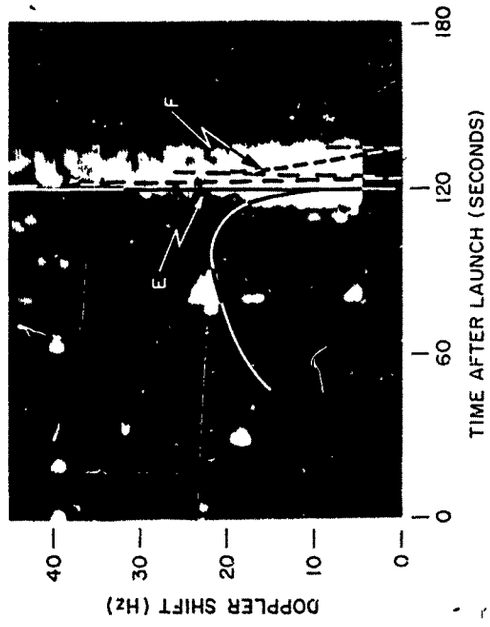

Fig. 33 - Observed signature for ETR launch 3670 compared with the E-layer (solid curve) and F-layer (dashed curve) unmatched simulations from Ref. 1 (S)

has reduced this error but has not removed it completely except at the expense of precision in later-time missile signature prediction. That errors in missile signature prediction cannot be completely removed by these means when ionospheric layer patchiness or other local effects exist is to be expected. The improvement in signature synthesis which results from this procedure is evident, however.

CONCLUSIONS (U)

(S) All in all, the backscatter-matching procedure described in this report can be seen to improve the first-iteration procedure described in Ref. 1. The evidence presented here suggests that it is of value in predicting signature onset more precisely than the former method. However, a major deficiency of this technique is its inability to account fully for local inhemogeneities in the layer structure. The occurrence of sporadic-E patches is an evident corruptor of the procedure described in this report. This type of insufficiency is an inevitable result of the use of diagnostic data which are integrated over a large volume of ionosphere to predict the behavior of a series of essentially point-to-point paths within that volume. Some improvement can be achieved by using a wide-aperture antenna for radar illumination of both the backscattering region of the earth and the target of interest. Additional improvement may be expected from the use of a larger sample of ionospheric sounding data along the path, together with a more sophisticated, two- or three-dimensional ray tracing approach. However, this additional improvement not only is expensive but cannot be expected to be accomplished on a real-time basis so that it may be included in an operational system.

(S) Several suggestions for the use of a near-real-time ionospheric ray tracing technique in conjunction with an operational over-the-horizon radar appear in Ref. 1. Modern signal-processing, automatic data-handling, and automatic radar and ionosonde control techniques can be used to perform a continuously updated ionospheric ray tracing and backscatter-matching process, whose result could be used with known performance characteristics of the expected missile targets to generate expected missile signatures. These synthesized signatures could be compared with observed missile-launch radar data to acquire estimates of trajectory parameters.

(S) Figure 34 illustrates an arrangement by which a rapid version of the ray tracing procedure described in this report might be used to perform this function. Earth backscatter data from an over-the-horizon radar, together with ionospheric sounding data

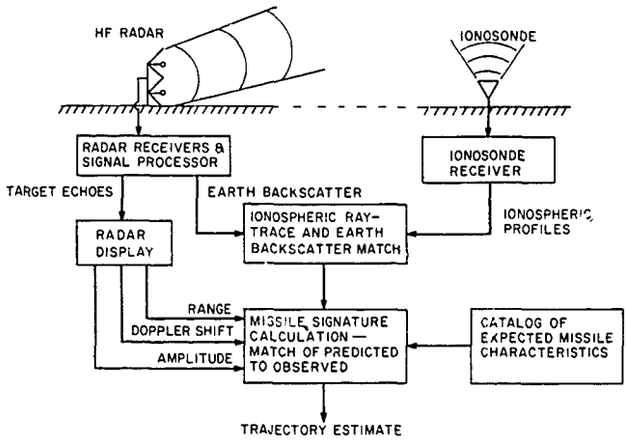

Fig. 34 - Possible implementation of backscatter-matching and missile signature simulation as a near-real-time process for an operational over-the-horizon radar (S)

from ionosondes located along the propagation path, would be processed by a computer to synthesize an earth backscatter distribution, compare it to an observed version, and construct a corrected ionospheric electron density profile. A hybrid computer could be used, with digital input, output, and control functions, to accomplish this time-consuming portion of the task most rapidly. The ray trace which results could be updated as often as changes in ionospheric conditions dictate, although it might be expected that each version would remain usable for some tens of minutes on the average.

(S) A catalog containing known performance characteristics of likely hostile targets could be used in a second step of the process, together with observed target data from the radar itself, to match an observed signature with a prediction based upon the stored ray-trace and variable trajectory parameters. The particular parameters required to achieve this match would then represent an estimate of the trajectory itself, from which estimates of likely launch and target regions, time of flight, and other useful quantities can be made.

REFERENCES (U)

1. Davis, J.R., Harding, M.E., Willis, J.W., and Utley, F.H., "Applications of Computer-Aided Ionospheric Ray Tracing Techniques to the Analysis of Over-the-Horizon Radar Signatures from Launch-Phase Rockets," NRL Report 6731 (Secret Report, Unclassified Title), July 30, 1968

2. Lucas, D.L., and Haydon, G.W., "Predicting Statistical Performance Indexes for High Frequency Ionospheric Telecommunications Systems," ESSA Technical Report IER-1-ITSA, August 1, 1966

DOCUMENT CONTROL DATA - R & D

Security classification of title, body of abstract and indexing annotation must be entered when the overall report is classified)

1 ORIGINATING ACTIVITY (Corporate author)
Naval Research Laboratory

2a. REPORT SECURITY CLASSIFICATION
SECRET

2b GROUP
3

3 REPORT TITLE
IONOSPHERIC EARTH BACKSCATTER SIMULATION APPLIED TO OVER-THE-HORIZON RADAR

4 DESCRIPTIVE NOTES (Type of report and inclusive dates)
An interim report on a continuing problem

5 AUTHOR(S) (First name, middle initial, last name)
John R. Davis, Frank W. Chambers, Edwin L. Althouse, and John W. Willis

6 REPORT DATE	7a TOTAL NO OF PAGES	7b. NO OF REFS
March 20, 1969	36	2

8a CONTRACT OR GRANT NO	9a. ORIGINATOR'S REPORT NUMBER(S)
NRL Problem R02-23	NRL Report 6866
b PROJECT NO: USAF MIPR FD2310-7-0016	
c	9b OTHER REPORT NO(S) (Any other numbers that may be assigned this report)
d	

10 DISTRIBUTION STATEMENT
In addition to security requirements which apply to this document and must be met, it may be further distributed by the holder ONLY with specific prior approval of the Director, Naval Research Laboratory, Washington, D.C. 20390

11 SUPPLEMENTARY NOTES	12 SPONSORING MILITARY ACTIVITY
	Department of the Air Force (Rome Air Development Center), Griffiss Air Force Base, Rome, N.Y. 13442

13 ABSTRACT (Secret)

A precision ionospheric ray-tracing technique has been developed to predict in detail the distribution of earth backscatter measured by a high-frequency over-the-horizon radar. A first-generation version of this technique was reported in NRL Report 6731. By making use of observed earth-backscatter distributions, in conjunction with ionospheric sounding data, it has been possible to refine the ray-tracing technique and improve its performance in predicting signatures of over-the-horizon rocket launches. In particular, it has been possible to predict the time of signature onset more precisely with these improvements.

This ray-tracing technique could be used in an operational over-the-horizon radar to provide, in near real time, estimates of trajectory parameters for actual hostile missile launches. Implementation of this capability in an operational radar would require the use of a sophisticated hybrid (digital/analog) computer as an integral part of the radar controller and signal processor.

14 KEY WORDS	LINK A		LINK B		LINK C	
	ROLE	WT	ROLE	WT	ROLE	WT
Radar						
High frequency						
Over-the-horizon radar						
Analysis						
Earth backscatter						
Simulation						
Ionosphere						
Computer routines						
Ray tracing						
Radar signatures						
Rocket launches						

MEMORANDUM

20 February 1997

Subj: Document Declassification

Ref: (1) Code 5309 Memorandum of 29 Jan. 1997
(2) Distribution Statements for Technical Publications NRL/PU/5230-95-293

Encl: (a) Code 5309 Memorandum of 29 Jan. 1997
(b) List of old Code 5320 Reports
(c) List of old Code 5320 Memorandum Reports

1. In Enclosure (a) it was recommended that the following reports be declassified, four reports have been added to the original list:

Formal: 5589, 5811, **5824**, 5825, 5849, 5862, 5875, 5881, 5903, 5962, 6015, 6079, 6148, 6198, 6272, 6371, 6476, 6479, 6485, 6507, 6508, 6568, 6590, 6611, 6731, 6866, 7044, 7051, 7059, 7350, 7428, 7500, 7638, 7655. Add **7684**, **7692**.

Memo: 1251, 1287, 1316, **1422**, [redacted], 1500, 1527, 1537, 1540, 1567, 1637, 1647, **1727**, **1758**, 1787, 1789, 1790, 1811, 1817, 1823, **1885**, 1939, **1981**, 2135, 2624, 2701, 2645, 2721, 2722, 2723, 2766. Add **2265**, **2715**.

The recommended distribution statement for the these reports is: **Approved for public release; distribution is unlimited.**

2. The above reports are included in the listings of enclosures (b) and (c) and were selected because of familiarity with the contents. The rest of these documents very likely should receive the same treatment.

J. M. Headrick
Code 5309

Copy:
Code 1221 — CR OK 7/2/97 —
Code 5300
Code 5320
Code 5324